Variation of fundamental and higher-order Raman spectra of ZrO_2 nanograins with annealing temperature

G. G. Siu and M. J. Stokes
Department of Physics and Materials Science, City University of Hong Kong, Tat Chee Avenue, Kowloon, Hong Kong, China

Yulong Liu
Institute of Physics, Chinese Academy of Sciences, P.O. Box 603, Beijing 100080, People's Republic of China
(Received 7 April 1998; revised manuscript received 24 June 1998)

ZrO_2 nanograins annealed at different temperatures are systematically investigated using x-ray diffraction (XRD) and Raman spectroscopy. Our results show that bulk properties of nano-ZrO_2 diminish but the defect-, surface-, and size-related features display as grain size decreases. A critical size that divides respective predominance is determined to be about 15 nm. Both XRD and Raman spectra of nano-ZrO_2 of size above 15 nm are similar to bulk ones. On the contrary, those of nano-ZrO_2 of size below 15 nm are deteriorated bulk spectra with spectroscopic line broadening and merging, line intensity reducing, and position shifting. Deteriorated XRD spectra are essentially associated with increasing defects in small nanograins. General mode softening, a surface mode around 1040 cm^{-1} and 14 weak second-order (overtone and combination) modes are characteristics of Raman spectra of nano-ZrO_2 below 15 nm. They are associated with microstructure change of nanograins, i.e., they reflect the effects of grain size, surface, and the interaction between nanograins.
[S0163-1829(99)02803-9]

I. INTRODUCTION

Nanomaterials have aroused great interest because of their unusual properties resulting from peculiar microstructure of nanograins, their basic construction units.[1,2] When the average grain size is controlled in the range of 1–100 nm, their physical and chemical properties can be significantly different from those of bulk materials owing to space confinement and surface effects.[3,4] It is important to understand the manner in which the structures and properties of a single nanograin vary with grain size, from atomic behavior to bulk solid-state behavior. Nanomaterials synthesized by different methods could have different microstructures such as nanocrystallite, nanoamorphous grain, or nanoclusters assembles with some crystal feature, which underlie their physical and chemical properties. It is essential to study the relationship of internal microstructure of nanograins with grain size for understanding physical mechanisms involved in nanomaterials and cooperative atomic phenomena such as lattice vibration.

The size of nanograins can be controlled by annealing nanomaterials. Their structures and the approximate mean size are conventionally determined by x-ray diffraction (XRD). A few papers have recently reported detailed XRD studies of the lattice distortion in nanomaterials and the microstructure changes with annealing temperature.[5,6] The vibrational properties of nanomaterials, which are strongly dependent on the nanograin size, are usually studied by Raman spectroscopy, which is a powerful characterization technique concerning molecular vibrations and dynamical properties of materials. We intend to combine these techniques and correlate their results.

Zirconium oxide (ZrO_2) is a useful functional material in high-temperature optical and electronic technologies,[7] and is also a typical material in structural-phase transitions because ZrO_2 can exist in several polymorphs.[8] There is a lot of work performed using IR,[9,10] and Raman[8,11] techniques to characterize the structures and properties of ZrO_2. In this paper, x-ray spectroscopy in range $2\theta = 10° - 80°$ and Raman spectra over a large frequency range 80–1250 cm^{-1} are measured systematically for ZrO_2 nanograins of the size ranging from 5 nm to 1 μm at room temperature. Compared with previous papers,[12,13] our results are improved and complete in the sense that additional vibrational modes of nano-ZrO_2 can be resolved together with a characteristic mode around 1050 cm^{-1} (a surface vibrational mode). These results provide useful information for studying the relationship between the grain size, the microstructure of nanograins and their vibrations.

II. EXPERIMENT

ZrO_2 nanograins of average diameter ~5 nm were prepared using the hydrothermal method from a solution of 1N zirconium nitrate in 2N nitric acids (N for normality concentration) after heating to 150 °C for 12 h in a sealed hyperbaric vessel cushioned with polytetrafluoroethylene, and then cooled to room temperature. White ZrO_2 powder was obtained after washing the product alternately and repeatedly with water and absolute acetone, which was dried in a vacuum desiccate for 14 h. ZrO_2 nanograins of different size were obtained by annealing the powder at different temperatures for 8 h. A series of annealing temperatures were chosen: 200 °C, 300 °C, 450 °C, 500 °C, 800 °C, and 1100 °C. The powders were compressed under 10 GPa into circular pieces of diameter ~10 mm and thickness ~1 mm.

An x-ray diffractometer (Rigaku D/Max-r) was used for structure identification with Cu $K\alpha$ radiation. The operating voltage and current were 50 kV and 200 mA, respectively. A transmission electron microscope (TEM, Hitachi 900) was

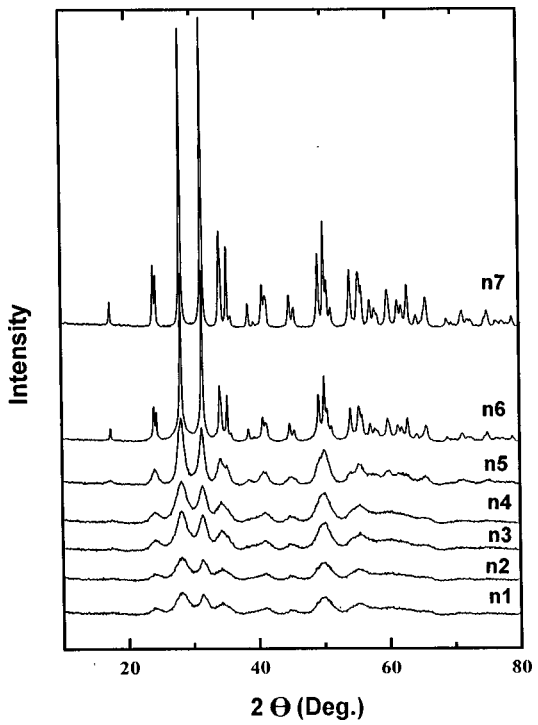

FIG. 1. XRD spectra of nano-ZrO_2 with different annealing temperature T_a:$n1$, as-grown sample; T_a=200, 300, 450, 500, 800, and 1000 °C, respectively, from $n2$ to $n7$.

used to take feature micrographs. The average size of ZrO_2 nanograins was determined by XRD and TEM. Two Raman spectrometers were used for investigating the vibrational modes of ZrO_2 nanograins at room temperature. One was a SPEX-1403 Ramalog system together with an argon ion laser (Coherent Innova-100), which provided 514.5- and 488.0-nm lines for excitation. Another was a Bruker 100 system, a near infrared (NIR) Fourier transform (FT) Raman spectrometer with a cw diode-pumped Nd:YIG (yttrium indium-garnet) laser for 1.06-μm excitation and with a liquid-nitrogen-cooled germanium detector. Backscattering geometry is adopted for all Raman measurements. In general, Raman spectra were collected under the conditions of laser power 50 mw and resolution 4 cm^{-1}. Typically 2500 scans at 4 cm^{-1} interval were averaged to provide a spectrum of sufficient quality. Results from two spectrometers are similar and only the NIR-FT Raman results are shown.

III. RESULTS AND DISCUSSION

Figure 1 is the XRD spectra of nano-ZrO_2 with different annealing temperatures, which shows that the samples are single-phase ZrO_2 with monoclinic structure. The average grain sizes are obtained from the Scherrer equation[14]

$$D = K\lambda/(\beta \cos \theta), \tag{1}$$

where D is the crystallite size, K a proportional constant, λ the wavelength of the x rays, β is the full width at half maximum (FWHM) of the diffraction peak in unit of radian, and θ is the Bragg angle. The results are given in Table I, which agree well with those from TEM studies.[5] The increase in grain size as $T_a \leqslant 500$ °C is moderate, which manifests that low-temperature annealing mainly removes the interface stress and effects the interface-structure relaxation. After 500 °C the grain size increases rapidly when annealing mainly causes grain growth.

TABLE I. The average grain sizes of nano-ZrO_2 annealed under different temperature.

Sample	$n1$	$n2$	$n3$	$n4$	$n5$	$n6$	$n7$
T_a (°C)	as-grown	200	300	450	500	800	1100
D (mm)	5.0	8.0	12	15	20	75	120

From $n1$ to $n7$ the grain size increases and correspondingly their XRD peaks are sharpening and resolving into fine structure. The as-grown sample $n1$ has eight broad diffraction peaks situated in the similar ranges of the monoclinic polycrystalline ZrO_2 spectrum. However, the bandwidths are large (so that the resolution is low), the positions shift, and the relative intensities are different from the literature data.[15] It is a deteriorated bulk spectrum, which is closely related to the fact that the presence of large numbers of lattice vacancies and local lattice disorders may result in considerable reduction in intensity and even lead to near disappearance of XRD peaks of crystal planes. The as-grown nanograins possess maximum structure disorders: oxygen vacancies, local lattice disorder, cluster pores, and etc. The smallest grain size also means the largest grain surface. There are huge numbers of interfaces between and inside nanograins so that many atoms or molecules of nanograins are in the surface or near-surface states. Therefore the $n1$ spectrum is the least bulk-like. There is no drastic change in the positions and intensities of XRD peaks from $n2$ to $n5$, although a tendency towards stronger peaks is apparent. It is consistent to the explanation that annealing under $T_a \leqslant 500$ °C is able to re-

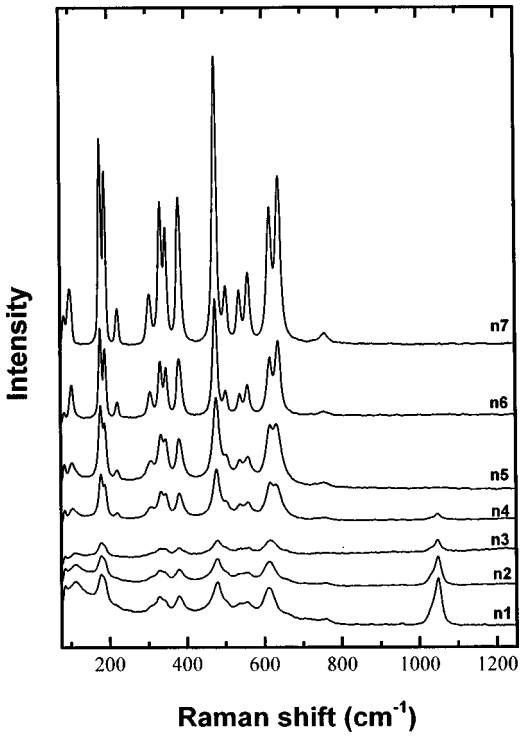

FIG. 2. Raman spectra of nano-ZrO_2 with different annealing temperatures ($n1$–$n7$).

TABLE II. Wave numbers (cm^{-1}) of the *C* group Raman modes of nano ZrO_2. (vs, very strong; s, strong; m, medium; w, weak; sh, shoulder; *, observed ambiguity; *T*, tetragonal phase. The modes with Raman shift larger than 700 cm^{-1} belong to the *H* group.)

*n*1	*n*2	*n*3	*n*4	*n*5	*n*6	*n*7	Ref. 8	Ref. 11
								92*
114 m	112 m	110 m	107 m	105 m	104 m	101 (A_g) m		101
								148^T
178 s	178 s	178 s	178 s	178 s	178 s	178 (A_g) s	179 (A_g)	177
		189 sh	190 s	191 s	191 s	191 (A_g) s	190 (A_g)	189
220 sh	220 sh	220 sh	220 sh	220 w	224 m	224 (B_g) m	222 (B_g)	222
							270^T	266^T
			308 sh	305 m	305 m	306 (A_g) m	305 (A_g)	306
								315*
328 m	330 m	332 m	334 m	334 m	334 s	334 (B_g) s	334 (B_g)	335
338 sh	340 sh	342 sh	345 sh	346 m	349 m	350 (A_g) s	348 (A_g)	347
								355*
380 m	380 m	380 m	381 m	382 m	382 s	382 (B_g) s	381 (B_g)	382
479 m	479 m	479 m	478 s	476 vs	475 vs	475 (A_g) vs	476 (A_g)	476
			501 sh	501 w	504 m	504 (B_g) m	500 (B_g)	502
534 sh	534 sh	534 sh	534 sh	536 w	539 m	539 (B_g) m	534 (B_g)	537
554 w	556 w	558 w	558 m	558 m	558 m	560 (A_g) m	557 (A_g)	559
612 m	612 m	616 m	616 s	616 s	618 s	618 ($2B_g$) s	615 ($2B_g$)	616
			633 sh	633 s	637 s	638 ($2A_g$) s	637 ($2A_g$)	637
704 w								
714 w								
725 w								
760 w	758 w	758 w	756 w	756 w	758 w	758 w	780	764

move stress and lead to relaxation in the interface structure, but is difficult to eliminate local lattice disorders or to change the internal structure of nanograins owing to their requirement for higher energy. The spectra of *n*6 and *n*7 are much bulklike, qualitatively different from the previous ones. The diffraction peaks sharpen, strengthen, and can be indexed according to the standard monoclinic structure. It shows that the grains have improved greatly. The rapid increase in grain size as $T_a > 500\,^{\circ}C$ is accompanied with a rapid decrease in the density of vacancies, local lattice disorders, and clusters pores.

Bulk ZrO_2 is monoclinic, belonging to the space group C_{2h}^5 ($P2_1/c$). A unit cell contains four formulas. Its vibration properties have been investigated.[11] According to group theory, there are 36 lattice vibrational modes:

$$G_{\text{mono}} = 9A_g + 9A_u + 9B_g + 9B_u \tag{2}$$

among which $9A_g$ and $9B_g$ modes are Raman active, while $8A_u$ an $7B_u$ modes are infrared active and others are acoustic modes.

The NIR-FT Raman spectra of nano-ZrO_2 with grain size ranging from 5 to 120 nm ($n1-n7$) are shown in Fig. 2, which are similar using 514.5 and 488.0 nm beam for excitation. To compare with published data, Table II lists the Raman frequencies of nano-ZrO_2 together with the frequencies of the ZrO_2 modes given in other sources.[8,11] For the sample *n*7 annealed at 1100 °C (the grain size is larger than 120 nm), our results are similar to Refs. 8 and 11 and can be interpreted based on the single-crystal or polycrystalline spectrum. There is no vibrational mode at 148 cm^{-1} or 266 cm^{-1} in any sample, which are attributed to the tetragonal phase.[8,11] The *n*6 spectrum is similar to *n*7 but the spectra from *n*1 to *n*5 are deteriorated bulk spectra with new features. These results indicate that the samples are basically single-phase ZrO_2 of monoclinic structure, in good agreement with XRD.

In Fig. 2, the Raman modes display usual anharmonic effects as the grain size decreases. Broadening, peak merging, and frequency shifting are observed. There are also some new features in the spectra. For example, an additional Raman mode, denoted as *S*, at 1038 cm^{-1} appears in the spectra of samples $n1-n5$ as the grain size is under 20 nm, which has asymmetric broadening on the low-frequency side of the peak. *S* strengthens and shifts toward higher frequency (1050 cm^{-1}) as the grain size decreases. Furthermore, 15 weak modes are observed in the sample *n*1 of grain size 5 nm.

It is noteworthy that the Raman spectra of nano-ZrO_2 vary systematically with grain size in the mode position, linewidth, and intensity. Their general behavior divides into three categories: Group *C* includes lines in the region 100–700 cm^{-1}; line *S* varies in the range 1030–1050 cm^{-1}; and Group *H* concerns the weak features in the region 700–1250 cm^{-1}. The spectral lines in Group *C* strengthen and resolve into sharp peaks with increase of grain size, following the evolution tendency of the XRD spectra. On the contrary, the line *S* and Group *H* behave oppositely and the Group *H* is very weak.

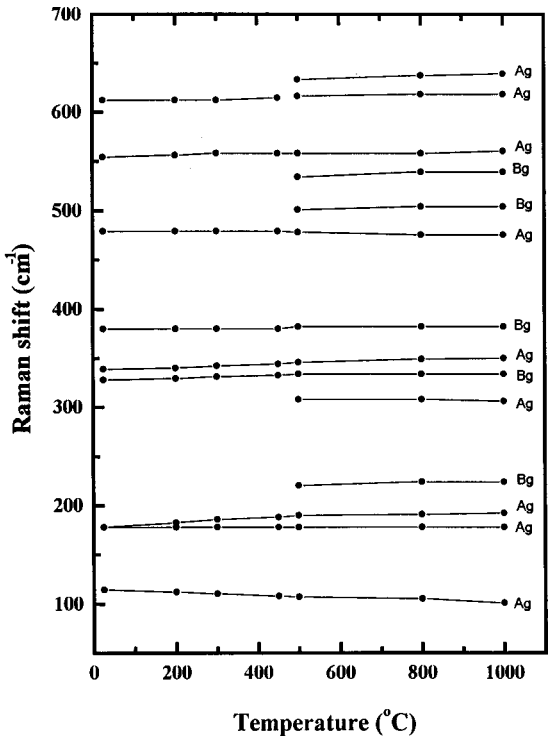

FIG. 3. Raman-mode wave numbers as functions of annealing temperature.

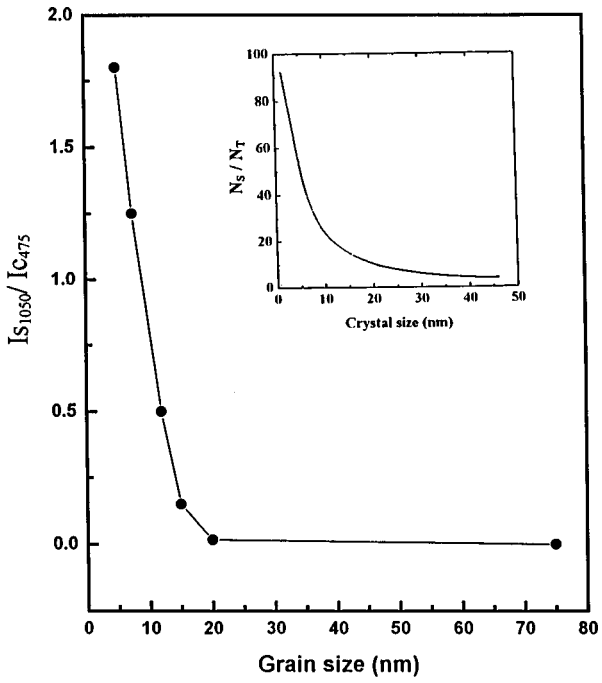

FIG. 4. $I_{S_{1050}}/I_{C_{475}}$ versus grain size.

The sample $n7$ has a bulk vibrational spectrum of monoclinic ZrO_2 crystal. The spectrum deteriorates continuously from $n6$ to $n1$, in the region of Group *C*. Each mode is denoted by its wave number as subscript. Their Raman shifts are listed in Table II where each row shows the variation of a mode frequency with grain size. The tendency of frequency shifting is clearly shown by Fig. 3, a graph of mode frequency versus annealing temperatures where each row of Table II becomes a line. The frequency variation is usually several cm^{-1} and red shift with grain-size reduction is common but blue shift also occurs. As grains contract, lines broaden and some merge with each other. In the meantime, the relative intensities of Raman modes also change. For example, the A_g modes C_{178} and C_{191} of $n7$ attenuate about twofold towards $n1$ and merge into a broad peak C_{178} of $n1$. C_{178} is stationary but C_{191} shifts to 178 cm^{-1} of $n1$, with a redshift as large as 13 cm^{-1}. Its FWHM almost doubles. Another example is the A_g mode C_{475} of $n7$, the strongest in the spectrum, which weakens to being similar to others towards $n1$. We conclude that Group *C* concerns bulk phonons and manifests the persistence of the basic polar-mode properties of the single crystal in nanograin.

The behavior of Group *C* shows clearly the dependence of Raman scattering by polar modes in a collection of randomly oriented crystallites on the size of the individual crystallites, as summarized in the Chapter 4 of Ref. 16. Similar behavior appears in $LiIO_3$ powder. Gualberto and Argüello obtained a good agreement between the experimental results and theoretical calculation of the spectral differential cross section of $LiIO_3$ powder.[17] Otaguro *et al.* studied the orientation dependence of the single-crystal polar-mode frequencies of $LiIO_3$ in the similar frequency range.[18] The details of the powder spectra are quite different from the single-crystal spectrum: not all the single-crystal peaks appear in the powder spectra and some that do appear are displaced in frequency and changed in intensity. The powder ones shows a continuous distribution over the range of the single-crystal polar-mode frequencies. Systematic change in grain size makes the tendency in spectral change clear.

The mode S_{1050} is the characteristic of $n1$. Single-crystal or polycrystalline ZrO_2 does not have any *S* mode, which appears only in ZrO_2 nanograins of small grain size ($\leqslant$15 nm). Figure 2 shows that the intensity of *S* drops as nanograins grow. *S* disappears completely when grain size reaches 50 nm. The grain-size dependence of the *S* intensity relative to that of C_{475} of $n1$ is shown in Fig. 4. The ratio of the number of superficial atoms N_S to the total number of atoms N_T versus grain size following Ref. 19 is plotted in the inset. Both increase rapidly when particle size decreases below 15 nm, suggesting some inner link. However, they have different coordinates scale (relative intensity and percentage) and I_{S1050}/I_{C475} has a dramatic drop for a diameter larger than 15 nm but the ratio N_S/N_T is a smoothly and slowly varying function, which make them dissimilar. It would not be possible to draw causal relation from comparison between two. On the other hand, this behavior is similar to the Raman spectra of small particles of silicon.[20] *S* mode behaves similarly to the Raman-scattering cross section of surface phonon in very small GaP spherical crystals calculated by Ruppin.[21] As the bulk-mode transverse and longitudinal cross sections of GaP sphere keep almost the same when sphere size changes, the surface-mode cross section exceeds them for sphere diameter smaller than about 20 nm, becomes comparable with the bulk-mode scattering for sphere diameter $\sim$100 nm and drops dramatically to being negligible for diameter $>$200 nm. The predominance of the surface-mode scattering at extremely small size in the order of magnitude of sphere diameter $\sim$20 nm is the most striking modification of the spectral results. The basic reason why the powdered specimen show new spectral features is that the wave-vector

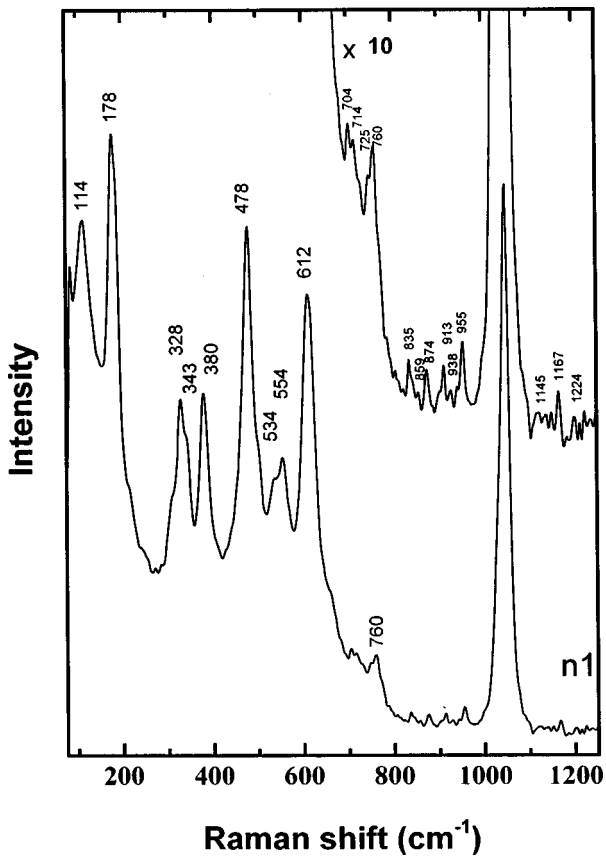

FIG. 5. Fundamental and higher-order Raman spectra of as grown nano-ZrO_2 over the range 80–1250 cm^{-1}.

conservation condition no longer limits the modes that contribute to light scattering when the particle size D is so small that $Dq \leqslant 1$, where $\hbar q$ is the momentum transferred.[16,18] For visible incident light of a typical wavelength ~514 nm (the green light of Ar^+ laser) into a crystal of refractive index ~1.5, its wave vector $\sim 1.8\times 10^7$ m^{-1} so that the maximum $q \sim 3.6\times 10^7$ m^{-1} (Ref. 16) and D would be smaller than ~30 nm. Hayes and Loudon,[16] however, pointed out that the scattering is nevertheless difficult to observe, and the crystallite in real powders are not usually spherical or even ellipsoidal, but have irregularities that broaden the surface-mode peak. Systematic reduction in size of nano-ZrO_2 provides an opportunity to observe the emerging and development of the surface-mode peak. We attribute S mode to surface-mode scattering, which is another observed surface phonon in addition to one from scattering by CdS crystallites.[22]

Figure 2 also shows that the mode S blueshifts from 1040 cm^{-1} ($n4$) to 1050 cm^{-1} ($n1$). It seems to be tempting to attribute this blue shift to quantum-size-effect related mechanism such as the surface electron-phonon interaction. A nanocrystal exciton model has been used to explain the blue shift of the absorption edge in photoacoustic spectrum and the absorption peaks of first-order differential PAS of nano-ZrO_2,[5] which was used in previous Raman-scattering work, too.[12] However, this interpretation of the blueshift of mode S is not convincing. By the spheroid model of nanoclusters, the energy of the exciton ground state of nano ZrO_2 can be expressed as[23]

$$E = E_g + \frac{\hbar^2\pi^2}{2R^2}\left(\frac{1}{m_e}+\frac{1}{m_h}\right) - 1.786\frac{e^2}{\varepsilon R} - 0.248E^*_{\mathrm{Ry}}, \quad (3)$$

where R is the radius, ε is the dielectric constant, m_e and m_h are the effective masses of the electron and the hole, respectively, and E_{Ry} is the effective Rydberg energy. On the right-hand side, the first term is the energy gap, the second is the quantum-size energy of localization, the third is the Coulomb interaction energy, and fourth results from the spatial correlation effect. The first term is constant and the fourth is independent of the size and usually small. The second ($\propto 1/R^2$) and third ($\propto 1/R$), respectively, represent an increase and a decrease in energy and are mutually canceling. The quantum size energy of localization will prevail as grain size decreases. When it dominates over the Coulomb energy, the excitation energy increases and could be higher than that of the eigenstate, which results in a blueshift of the peak. However, why should the energy of surface vibrations be related to the energy of an exciton? More relevant interpretation should relate the blue shift of surface vibration to surface itself. It results likely from surface relaxation as the particle size decreases. A surface optic phonon was observed on the TaC(100) surface by inelastic electron scattering[24] and for TaC with simple rocksalt crystal structure the dispersion curve of the surface mode on (100) can be calculated applying the diatomic linear-chain model.[25] The theoretical dispersion values based on this nearest-neighbor central-interaction model are smaller than the experimental ones because of modified force constants (surface relaxation) near the surface or owing to the effect of second- and third-neighbor forces. Although there is no simple theoretical model for the surface mode of monoclinic ZrO_2, similar change in force constants might occur owing to surface relaxation, which strengthens as the particle size decreases. Corresponding increase in force constants causes the blueshift.

Group H includes weak features at 704, 714, 725, 807, 835, 859, 874, 911, 928, 938, 955, 1145, 1167, and 1224 cm^{-1}, clearly observable in Fig. 5. They are sharp with Lorentzian line shape and linewidth in the region 10–20 cm^{-1}. Their frequencies are too high to be related to the first-order silent modes. They are likely the second-order active Raman modes. A Raman or infrared spectrum of a crystal (molecule) may contain numerous combination and overtone bands arising from anharmonicity. An ideal crystal has infinite spatial correlation length of phonon, and hence, the phonon eigenstates are plane wave. It leads to the usual selection rule, phonon momentum $q \cong 0$ for the first-order (the upper limit of q is three orders of magnitude smaller than the Brillouin-zone boundary) and $q + q' = 0$ for the second-order two-phonon (now phonon wave vectors q and q' are typically three orders of magnitude larger than the light wave vectors over the major part of the Brillouin zone) Raman scattering. The order of a real crystal, however, is not perfect owing to defects, impurities, disorder, etc. It means that the spatial correlation function of the phonon becomes finite in extent. It relaxes the selection rule, which, in turn, results in observation of symmetry-forbidden modes, together with line broadening and asymmetry of line shape, as well as redshifting of phonon mode. A combination band belongs to the direct product of representations to which the internal fundamental vibrations belong and its observed frequency is

TABLE III. Wave numbers (cm^{-1}) of the *H* group, Raman combinations and overtones, in $n-1$.

Mode	Position	Combination	Error
*H*1	704	328+380	4
*H*2	714	534+178	−2
*H*3	725	612+114	1
*H*4	807	328+479	0
*H*5	835	612+220	−3
*H*6	859	380+479	0
*H*7	874	534+343	3
*H*8	913	534+380	−1
*H*9	938	328+612	2
*H*10	955	478+478	1
*H*11	1145	534+612	1
*H*12	1167	554+612	−1
*H*13	1224	612+612	0

the sum of their frequencies.[26] For overtone bands, the characters of vibration representations are given by[27,28]

$$\chi_{f2}(R)=[\chi_f(R)]^2, \quad \text{for } f=1,$$

$$\chi_{f2}(R)=(1/2)\{[\chi_f(R)]^2+\chi_f(R^2)\}, \quad \text{for } f\geqslant 2, \qquad (4)$$

where $\chi_f(R)$ is the character under the operation R for the f-fold degenerate irreducible representation ir of the point group, and $\chi_{f2}(R)$ is the character of the reducible representation of the first-order overtone whose fundamental vibrations belong to f-fold degenerate ir. These bands have well-defined frequencies and widths in the same order of magnitude as the fundamental bands. In these cases, predictions from selection rules based on the factor group are generally sufficient.[26,29] Higher-order Raman modes are usually very weak, e.g., the intensity of second-order Raman modes is about one or two orders of magnitude smaller than that of their fundamental modes. Figure 2 gives the ratio of intensities $I_{478}/I_{956}=22$. The higher-order Raman modes in $n1$ are listed in Table III, in good agreement with quantum theory. The appearance of high-order modes in Raman spectra of nano-ZrO_2 brings new possibility for studying the microstructures of nanograins because the selection rules of high-order modes are different from those of fundamental modes.

In summary, sample $n5$ distinguishes between the samples that show noteable ''size+interface'' effects and the samples in which bulk properties predominate. Its surface mode *S* and Group *H* almost disappear and its bulk phonon modes start to intensify, showing reduction of the lattice vacancies and local lattice disorder. Correspondingly, its lattice distortion weakens and all XRD peaks start to strengthen. Nanograin samples show bulklike spectra as $D>15$ nm, which manifests grain growth improves crystallite quality. Samples of $D\leqslant 15$ nm, on the contrary, show deteriorated bulk spectra with clear ''finger print'' of size and interface effects.

IV. CONCLUSIONS

We have systematically measured XRD and Raman spectra of ZrO_2 nanograins of size in the region 5–120 nm at room temperature. Both the structure and vibration of nanograins of size under 15 nm show characteristics different from bulk ones. Their essentially monoclinic bulk properties diminish. Their spectral-line weakens, broadens, and merges. In Raman spectra shifts of modes are common, an extra surface vibrational mode *S* around 1040 cm^{-1} and weak second-order Raman modes (Group *H*) appear. The results show the effects of defects, size and interfaces in typical ZrO_2 nanograins. On the other hand, nanograins of size above 20 nm are very similar to bulk solids. The bulk characteristics recover in both spectra, showing the predominance of interior order. It suggests that the modes *S* and Group *H* are closely related to the change of nanograin microstructure.

[1] H. Gleiter, Nanostruct. Mater. **1**, 1 (1992).
[2] R. W. Cahn, Nature (London) **348**, 389 (1990).
[3] J. Karch, R. Birringer, and H. Gleiter, Nature (London) **330**, 556 (1987).
[4] R. E. Sherriff and R. P. Devaty, Phys. Rev. B **48**, 1525 (1993).
[5] Y. H. Xiong, K. N. Yu, and C. S. Xiong, Phys. Rev. B **49**, 5607 (1994).
[6] J. A. Eastman, J. Appl. Phys. **75**, 770 (1994).
[7] A. Feinberg and C. H. Perry, J. Phys. Chem. Solids **42**, 513 (1981).
[8] C. Carlone, Phys. Rev. B **45**, 2079 (1992).
[9] Y. Ishikawa, R. Toarnier, and J. Filippi, J. Phys. Chem. Solids **26**, 1727 (1965).
[10] T. Hirata, Phys. Rev. B **50**, 2874 (1994).
[11] E. Anastassakis, B. Papanicolaou, and I. M. Asher, J. Phys. Chem. Solids **36**, 667 (1975).
[12] F. X. Liu, J. L. Yang, and T. P. Zhao, Phys. Rev. B **55**, 8847 (1997).
[13] Zhuo Jiang, Acta Opt. Sin. **12**, 946 (1992).
[14] B. D. Cullity, *Elements of X-ray Diffraction* (Addison-Wesley, London, 1959), p. 261.
[15] C. J. Howard, R. J. Hill, and B. E. Reichert, Acta Crystallogr., Sect. B: Struct. Sci. **44**, 116 (1988).
[16] W. Hayes and R. Loudon, *Scattering of Light by Crystals* (Wiley, New York, 1978).
[17] G. M. Gualberto and C. A. Argüello, Solid State Commun. **14**, 911 (1974).
[18] W. S. Otaguro, E. Wiener-Avnear, S. P. S. Porto, and J. Smit, Phys. Rev. B **6**, 3100 (1972).
[19] D. Feng, Y. N. Wang, and D. R. Qiu, *Metal Physics* (Science Publishing House, Beijing, 1964), p. 408.
[20] T. Okaola, T. Iwoki, K. Kasahara, and K. Abe, Solid State Commun. **49**, 809 (1984).
[21] R. Ruppin, J. Phys. C **8**, 1969 (1975).
[22] J. E. Scott and T. C. Damen, Opt. Commun. **5**, 410 (1972).
[23] Y. Kayanuma, Phys. Rev. B **38**, 9797 (1988).
[24] C. Oshima, R. Souda, M. Aono, S. Otani, and Y. Ishizawa, Phys. Rev. B **30**, 5361 (1984).
[25] M. G. Cottam and C. R. Tilley, *Introduction to Surface and Su-*

perlattice Excitations (Cambridge, New York, 1989), Chap. 2.
[26] H. Poulet and J. P. Mathieu, *Vibration Spectra and Symmetry of Crystals*, translated by A. Simievic (Gordon and Breach, New York, 1976).
[27] Von L. Tisza, Z. Phys. **82**, 48 (1933).
[28] M. Tinkham, *Group Theory and Quantum Mechanics* (McGraw-Hill, New York, 1964); E. B. Wilson, Jr., J. C. Decius, and I. C. Cross, *Molecular Vibrations—The Theory of Infrared and Raman Vibrational Spectra* (Dover, New York, 1980).
[29] Y. L. Liu, Y. J. Jiang, J. Q. Liu, and Y. J. Mo, Phys. Rev. B **49**, 5058 (1994).